

Summary Abstract: A theoretical analysis of the deactivation of metal surfaces upon carburization

S. A. Jansen and R. Hoffmann

Citation: *J. Vac. Sci. Technol. A* **5**, 637 (1987); doi: 10.1116/1.574654

View online: <http://dx.doi.org/10.1116/1.574654>

View Table of Contents: <http://avspublications.org/resource/1/JVTAD6/v5/i4>

Published by the AVS: Science & Technology of Materials, Interfaces, and Processing

Related Articles

Flash sample heating for scanning tunneling microscopy: Desorption of 1-octanethiolate self-assembled monolayers in air

J. Vac. Sci. Technol. B **31**, 013201 (2013)

New method of calculating adsorption and scattering for Xe-Pt(111) using Direct Simulation Monte Carlo techniques

J. Vac. Sci. Technol. A **30**, 061401 (2012)

Gain and loss mechanisms for neutral species in low pressure fluorocarbon plasmas by infrared spectroscopy

J. Vac. Sci. Technol. A **30**, 051308 (2012)

Differences in erosion mechanism and selectivity between Ti and TiN in fluorocarbon plasmas for dielectric etch

J. Vac. Sci. Technol. B **30**, 041811 (2012)

Investigation of interfacial oxidation control using sacrificial metallic Al and La passivation layers on InGaAs

J. Vac. Sci. Technol. B **30**, 04E104 (2012)

Additional information on *J. Vac. Sci. Technol. A*


Journal Homepage: <http://avspublications.org/jvsta>

Journal Information: http://avspublications.org/jvsta/about/about_the_journal

Top downloads: http://avspublications.org/jvsta/top_20_most_downloaded

Information for Authors: http://avspublications.org/jvsta/authors/information_for_contributors

ADVERTISEMENT




Aluminum Valves with Conflat® Flanges

Less Outgassing Than Stainless
Mate to Stainless Steel Conflats
Sizes From 2.75 to 14 inch O.D.
Leak Rate Less Than 10^{-10} SCC/S

Visit us
at Booth # 300
in Tampa

Prices & Specifications
vacuumresearch.com



and very high in energy, but the sulfur lone pair orbitals are only ~ 2 eV below the Fermi level. The projected DOS's indicate that for each of the geometries, the more important of the two is the one best able to interact with the Mo yz states. For the on-top geometries, the interaction is π bonding, involving $2b_1$ for the perpendicular site (1) and $9a_1$ for the parallel (3). The lone pair oriented radially, rather than tangentially, with respect to the Mo-S₂-Mo angle dominates the bridging modes [$9a_1$ for the perpendicular (4) and $2b_1$ for the parallel (6)]. A comparison of the dispersion and charge transfer out of the lone pairs shows that bridging thiophene is a superior electron donor to on-top thiophene. The direction of net charge flow is exclusively from the adsorbate to the substrate, and into the uncoordinated surface or bulk Mo atoms. Coordinated Mo atoms tend to be further oxidized. The most profound effect is the $+1.27$ charge at the η^5 Mo relative to the bare surface.

The sequential removal of three of the four sulfur neighboring a coordinated Mo atom bring out a problem inherent in noninfinite models, that being, what charge to assign to the nonstoichiometric unit cell. The problem will be addressed in more detail in a subsequent work. Regardless, the effect on the dispersion and distribution of the thiophene orbitals is significant in most coordination geometries. We discuss only the η^5 case here. As previously mentioned, the Mo xy becomes increasingly involved in backbonding. The important thiophene $3b_1$ and $2b_1$ become more compact as they interact with less diffuse Mo orbitals (fewer MoS₂ sur-

face bonds). Assuming a constant Fermi energy to circumvent the aforementioned charge problem leads to a slight increase in the $3b_1$ occupation ($\sim 5\%$ total) and decrease in the S-C o.p. ($\sim 10\%$ total).

Our extended Hückel calculations implicate η^5 -bound thiophene as a possible active species for HDS. Defect sites may be more reactive. Certainly more geometries must be explored before a definitive active site is discovered.

Acknowledgments: We wish to thank Suzanne Harris for helpful discussions, and the Office of Naval Research for their support of this work.

¹(a) M. Zdražil, *Appl. Catal.* **4**, 107 (1982); (b) F. E. Massoth, *Adv. Catal.* **27**, 265 (1978); (c) S. Harris and R. R. Chianelli, *J. Catal.* **86**, 400 (1984).

²(a) C. B. Roxolo, M. Daage, A. F. Ruppert, and R. R. Chianelli, *J. Catal.* **100**, 176 (1986); (b) J. Joffre, P. Géneste, and D. A. Lerner, *ibid.* **92**, 56 (1985).

³(a) D. A. Lesch and R. J. Angelici, *J. Am. Chem. Soc.* **106**, 2901 (1984); (b) C. A. Kuehn and H. Taube, *ibid.* **98**, 689 (1976).

⁴(a) F. Zaera, E. B. Kollin, and J. L. Gland (to be published); (b) (to be published).

⁵J. T. Roberts and C. M. Friend (to be published).

⁶R. H. Summerville and R. Hoffmann, *J. Am. Chem. Soc.* **98**, 7240 (1976).

⁷J. C. J. Bart and V. Ragaini, in *Proceedings of the Climax Fourth International Conference on the Chemistry of Molybdenum*, edited by H. F. Gray and P. C. H. Mitchell (Climax Molybdenum Co., Ann Arbor, MI, 1979), p. 19.

⁸M. C. Zonnevylle and R. Hoffmann (to be published).

⁹T. A. Albright, J. K. Burdett, and M. H. Whangbo, *Orbital Interactions in Chemistry* (Wiley, New York, 1985), p. 388.

Summary Abstract: A theoretical analysis of the deactivation of metal surfaces upon carburization

S. A. Jansen and R. Hoffmann

Department of Chemistry and Materials Science Center, Cornell University, Ithaca, New York 14853-1301

(Received 19 September 1986; accepted 8 December 1986)

I. INTRODUCTION

The catalytic activity of transition-metal surfaces can be altered significantly by the deposition of carbon adlayers.^{1,2} In the case of nickel surfaces, several catalytic processes are enhanced.^{3,4} For the case of tungsten, a reconstruction occurs and the resultant surface activity is associated with both structural and electronic changes induced by the deposition of carbon.^{5,6} Recent experimental studies on transition-metal carbides and carburized transition metals have suggested that the carbon, either present in the bulk or exposed at the surface, affects the adsorption properties of simple gaseous adsorbates. The studies on the transition-metal carbides are

of interest not only because of their intrinsic surface chemistry, but also because of their relevance to certain carbided surfaces. The following discussion focuses on two systems: TiC and WC. TiC has been the subject of scrutiny for years, as it exhibits remarkable physical properties.⁷ Recently, several experiments have been performed on the (100) and (111) faces of TiC, as this material shows several similarities to titanium metal without the same disposition toward corrosion. Similar experiments have been performed on NbC, showing parallel chemical tendencies.⁸ The calculations were performed on TiC; however, the general trends and conclusions obtained through the theoretical analysis are valid for either system. The analysis performed focuses on

the (100) and (111) faces, as these faces represent the extremes in reactivity. WC(0001) was selected for study, since this material serves as a tenable model for the $W(100)-(5 \times 1)-C$ surface. The properties of these surfaces have been evaluated in terms of simple gaseous adsorption and decomposition by the extended Hückel/tight-binding method.

II. SURFACES OF STUDY

A. TiC

TiC crystallizes in the rock salt structure with a Ti-C distance of 2.164 Å and Ti-Ti and C-C distances of 3.06 Å. Two faces have been successfully prepared, the (100) and (111), while attempts at preparation of the (110) face have provided only faceted surfaces. The (100) face is a square face in which both Ti and C atoms are exposed. The primary adsorption chemistry is affected by the presence of the surface carbon. The (111) face considered is a Ti terminated face. For the (100) face special consideration was given to the question of the effect of carbon vacancies at the surface. Figure 1(a) shows the TiC surfaces of interest to this study. (The bond distances and lattice constant for NbC are nearly identical to those of TiC.)

B. WC

Studies on WC (0001) are proposed to model those of the $W(100)-(5 \times 1)-C$ in which surface reconstruction provides for nearly hexagonal layers of tungsten at the surface. The carbon atoms form the second layer of the substrate, and are also nearly hexagonal. Ultraviolet photoemission spectroscopy studies have shown that the valence orbitals of the WC and the carbided tungsten surface are nearly identical.⁹ For these reasons, WC(0001) is selected as a suitable model for the carbided surface. The W-W distance is 2.900 Å and the W-C distance is 2.194 Å. Figures 1(b) and 1(c) show the structural similarities between the $W(100)-(5 \times 1)-C$ and WC (0001) surfaces.

III. CO ON TiC SURFACES

The adsorption of CO on TiC provides for an interesting study of the surface reactivity of related carbides and carburized surfaces. CO is known to dissociate on Ti (0001) surfaces.¹⁰ The C-O overlap population and $2\pi^*$ occupation reflect significant reduction of CO bond strength. At the same time, a large M-C overlap population is observed. Recent experimental studies have shown that CO dissociates on NbC(111), but is observed in both molecular and dissociative states on NbC(100). The dissociative states on NbC(100) are suspected to be due to carbon vacancies at the surface. Calculations on the (111) face have shown a sizable reduction in C-O overlap population, and a correspondingly large increase in the occupation of the $2\pi^*$ orbital. Table I shows the overlap population and fragment molecular orbital (FMO) populations for TiC(100), TiC(100) with carbon vacancies at the surface, and the (111) face.

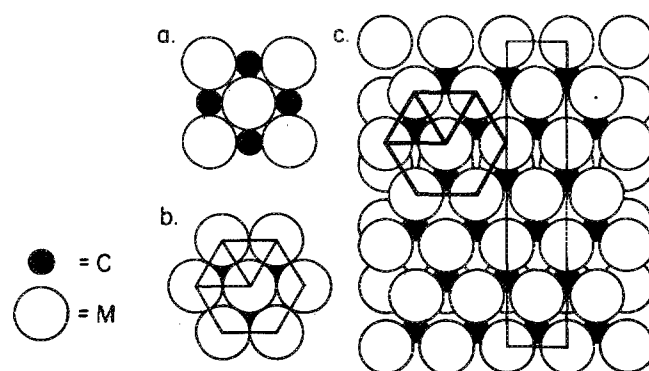


FIG. 1. (a) Top layer of the (100) face of TiC/NbC. (b) Top layer of the (111) face of TiC/NbC, showing the second layer of substrate carbon in alternating hollow sites. The same structure is observed for the top two layers of WC(0001). (c) The $W(100)-(5 \times 1)-C$ surface, showing the (5×1) unit cell and the nearly hexagonal packing of W and C layers.

The calculations on the (111) face show many similarities to that of Ti(0001). The explanation for the increased reactivity of this face, relative to that of the (100) face, is twofold. First, the preparation of the (111) face provides for more dangling bonds or orbitals per surface atom than the (100) surface. Second, the M-C surface bonding is quite strong and occurs with significant charge transfer from the M *d*-block. This reduces the electron density at the metal, hence its donor properties with respect to the $2\pi^*$ orbitals of CO. This is consistent with experimental observations. For the (100) surface, the reactivity is greatly inhibited. The dissociative states of CO are associated with carbon vacancies at the surface.

The calculations on the (111) face show many similarities to that of Ti(0001). The explanation for the increased reactivity of this face, relative to that of the (100) face, is twofold. First, the preparation of the (111) face provides for more dangling bonds or orbitals per surface atom than the (100) surface. Second, the M-C surface bonding is quite strong and occurs with significant charge transfer from the M *d*-block. This reduces the electron density at the metal, hence its donor properties with respect to the $2\pi^*$ orbitals of CO. This is consistent with experimental observations. For the (100) surface, the reactivity is greatly inhibited. The dissociative states of CO are associated with carbon vacancies at the surface.

IV. OXYGEN CONTAINING ADSORBATES ON TiC

Methanol is known to adsorb molecularly on NbC(100) while a methoxy species is observed on the (111) face. A theoretical consideration of oxygen adsorption on these two surfaces has suggested adsorption sites for the study of methanol on these two surfaces.

Ion scattering spectroscopy experiments have shown a

TABLE I. Overlap population and FMO analysis for CO on selected surfaces of TiC.

| FMO occupations | TiC(100) | TiC _{0.5} (100) | TiC ₀ (100) | TiC(111) | Ti(0001) ^a |
|--------------------|----------|--------------------------|------------------------|----------|-----------------------|
| 5σ | 1.731 | 1.725 | 1.725 | 1.725 | 1.730 |
| 2π*/orbital | 0.132 | 1.380 | 1.530 | 1.430 | 1.610 |
| Overlap population | | | | | |
| C-O | 1.173 | 0.437 | 0.473 | 0.469 | 0.430 |
| M-C | 0.616 | 0.976 | 1.060 | 1.053 | 1.110 |

^aReference 11.

marked decrease in intensity in the peaks arising from the surface carbon, suggesting that the oxygen sits directly atop the carbon.¹² On TiC(111), the oxygen atom is believed to sit in a threefold hollow site. One other site has also been observed; however, this site is not well characterized, but is suspected to be a twofold bridging site. Calculations on the (111) face have shown that of the possible adsorption sites, a threefold hollow and twofold bridging site are energetically favorable. There is one other threefold site, in which a bulk carbon atom lies directly below the adsorbate. This site is not suggested for oxygen/methanol adsorption as the C–O interaction is antibonding, and hence increases the overall energy of adsorption. The M–O interaction is approximately the same as in the case of the other threefold hollow sites. The twofold bridging site is “stabilized” by a bonding interaction between the bulk carbon and bridging oxygen. The energies of the two preferred sites are approximately the same.

The sites considered for the discussion of methanol on these two surfaces will be those in which the O of the methanol adsorbate is “atop” the surface carbon on the (100) surface. For the (111), the site to be discussed is one suggested by Yates *et al.*¹³ for methanol on Ni(111). The methanolic oxygen occupies a twofold bridging site, while the proton is directed toward a threefold hollow site. This site is consistent with the studies of oxygen on the (111) face of TiC and also consistent with the observation of bridging atomic adsorbates when surface distances are relatively long. In the case of TiC(111), the shortest metal–metal distance is 3.06 Å. The coverage assumed for each surface is $\frac{1}{4}$, insuring no adsorbate–adsorbate interaction.

For methanol on the (100) face, there is some weakening of the O–H bond. However, there is a compensating C (surface)–H interaction which may stabilize the methanol on the surface. A comparison of both the bonding and energetics of methanol and methoxy moieties on this surface shows increased C–O interaction for the methoxy species, though no energetic preference is observed for methoxy over that of methanol. This suggests a tradeoff in bonding. In the case of methanol on the (100) face, the C–H interaction contributes to the overall stability of the adsorbate, though reducing the $C_{\text{surface}}\text{--O}$ and O–H interactions. The $C_{\text{surface}}\text{--O}$ overlap population has a value of 0.318 for methanol in this site. The value of methoxy similarly oriented with respect to the surface is 0.472. The C–O bond strength of methoxy or methanol is not affected upon adsorption. In the case of methanol, the overlap population between the surface carbon atom and the hydroxyl proton is 0.180, while the O–H bond has an overlap population of 0.480, relative to 0.600 observed for “free” methanol.

The decomposition of methanol into methoxy species on the (111) face of TiC/NbC is not easily or readily understood. A comparison of the interaction of both methoxy and methanol with the surface may provide some insight to the driving force for the deprotonation of methanol. In many cases the methanol is deprotonated upon adsorption, but is able to recombine such that the only desorption product is methanol, suggesting a delicate equilibrium between methanol and methoxy species. Calculations of methoxy and methanol on the (111) face have shown a large energetic preference for methoxy. This can be traced to stronger M–O and C–O bonding. In the case of methanol, only a small antibonding interaction is observed between the “exchangeable proton” and the substrate atoms. For methanol on this face, the Ti–O overlap population is 0.212, while that for methoxy adsorption is 0.369. The oxygen is multiply coordinated to Ti surface atoms so the increase in overlap population is quite substantial. Though the net bond order is small, the carbon in the substrate interacts in a bonding way with the oxygen in the case of methoxy adsorption, but in an antibonding way for methanol. The overlap populations for these interactions are 0.020 and –0.013, respectively. This value is critically dependent on the Ti–O distance selected, as this designates the C–O distance. The distance selected for the Ti–O distance is 1.9 Å, which is a typical Ti–O bridging distance. The hydroxyl proton does not interact with any substrate atoms in a significant way. The overlap population of the O–H bond is not reduced upon adsorption; however, the presence of the hydroxyl proton seems to reduce the Ti–O bonding. The binding energies of both adsorbates are favorable for adsorption, but that of methoxy is significantly higher as to suggest that deprotonated products are more stable at the surface.

V. CO AND HCN ON WC(0001)

Experimental studies on carbided tungsten have shown only one type of CO at the surface. CO on the pristine surface is known to adopt a variety of sites, of which at least one is dissociative. On the carbided surface, a single state of CO is observed in which the CO is believed to be molecular and in an atop site. The vibrational frequencies obtained from high-resolution electron energy-loss spectroscopy (HREELS) for α CO on W(100) and CO on the carbided surface is slightly less reactive than the pristine surface. The population of the 5σ orbital of CO on either surface is the same, 1.695 electrons. The population of the $2\pi^*$ orbital is slightly higher for the W(100) surface. Each $2\pi^*$ level of CO receives 0.650 electrons upon adsorption, giving a total popu-

TABLE II. Overlap populations and FMO analysis for dissociative modes of HCN on W(100) and WC(0001).

| FMO occupations | W(100) | WC(0001) | Overlap pop. | W(100) | WC(0001) | Reference |
|-----------------|--------|----------|--------------|--------|----------|--------------------------|
| 7a' | 0.695 | 0.718 | C–N | 1.278 | 1.422 | 1.681 |
| 2a" | 0.689 | 0.337 | C–H | 0.593 | 0.622 | 0.770 |
| | | | W–N | 0.100 | 0.135 | 0.555 atop HCN |
| | | | W–C | 0.348 | 0.010 | 0.417 W–C _{sub} |